# Axial Distribution of Solid Holdup in Bubble Column for Gas-Liquid-Solid Systems

The axial distribution of solid holdup was investigated in a bubble column of 0.07 m in diameter and 4.25 m in height. The particle phase was glass beads of diameter 66, 118, 243, 465 or 1,300 $\mu$m. The effective slip velocity and the axial dispersion coefficient of the solid particles were evaluated in batch operation without solids feed and were correlated on the basis of mixing length theory. The equations obtained were applied to analyze axial profiles of particle concentration with a continuous feed of solids, and experimental data in the literature were simulated successfully over a wide range of solid concentration.

**Toshitatsu Matsumoto**
**Nobuyuki Hidaka**
Department of Chemical Engineering
Kagoshima University
Korimoto, Kagoshima 890, Japan

**Shigeharu Morooka**
Department of Applied Chemistry
Kyushu University
Higashi-ku, Fukuoka 812, Japan

## Introduction

Three-phase bubble columns, in which solid particles are suspended by upward gas and liquid flow, have been used in many chemical processes. One of engineering concerns is the longitudinal distribution of particle concentration caused by the interaction between gravitational settling and turbulent mixing of solid particles in a column. Most investigators have applied a sedimentation-dispersion model to describe the axial profiles of solid concentration (Imafuku et al., 1968; Kato et al., 1972; Smith and Ruether, 1985; Morooka et al., 1986). Jean and Fan (1987) emphasized the effects of bubble-wake and particle interaction. None of the models used in previous works, however, can predict the whole axial profile of solid concentration in a column which consists of two zones, the three-phase fluidized region with a nearly constant solid holdup, and the freeboard region with a diminishing solid holdup.

In the present paper, the effective settling velocity and the dispersion coefficient of solids were measured in a long, vertical column for a three-phase system operated batchwise with respect to solids. The effects of gas and liquid velocities, particle size, and phase holdups are discussed on the basis of the mixing length theory. Axial profile data of solid holdup with continuous solid feed was then simulated by the newly proposed model with system parameters obtained in the batch experiment.

## Experimental Apparatus and Procedures

A schematic diagram of the experimental apparatus is shown in Figure 1. The fluidization column, made of transparent acrylic resin pipe with an inner diameter of 0.07 m and a height of 4.25 m, was set vertically. The gas distributor was a stainless steel spiral tube of 6 mm in outer diameter, with six 2-mm holes pointing downward, and was installed horizontally at 0.105 m above the bottom. The liquid distributor was a packed bed of 10-mm-dia. glass spheres, a bronze net of 145 mesh being placed at upper face of the bed. All the experiments were conducted batchwise with respect to the solid particles. To prevent the entrainment of particles from the column, a divergent section made of bronze net was provided at the top of the column.

The gas was air, and the liquid was tap water at room temperature. The solid phase was sieved glass beads (density = 2.5 $Mg/m^3$) of 66, 118, 243, 465 and 1,300 $\mu$m in diameter, and the amount of particles put in the column was changed depending on experimental conditions. The particle size distribution which was obtained by sizing more than 1,000 particles per each sample is illustrated in Figure 2.

The axial profile of solid holdup was measured by using ten shutter plates which could be slid air-tightly. The configuration was reported by Al-Dibouni and Garside (1979), Morooka et al. (1980), Kato et al. (1985), and Fan et al. (1987). Shutter plates were installed horizontally with a distance of 0.2 m and were interconnected with wire ropes. Immediately after the feeds of gas and liquid were stopped, the wires were pulled to the closed position. By this motion, the column was momentarily partitioned into 11 parts. The mean gas holdup was determined from the total gas volume trapped by the shutter plate, by measuring the height of the gas head space in each section after gas disengagement was allowed to occur. The solid holdup was calculated by withdrawing solids settled on each shutter plate through the solids withdrawing tap (Figure 1) and weighing them. The axial dispersion coefficient of liquid was determined by the impulse

Correspondence concerning this paper should be addressed to T. Matsumoto.

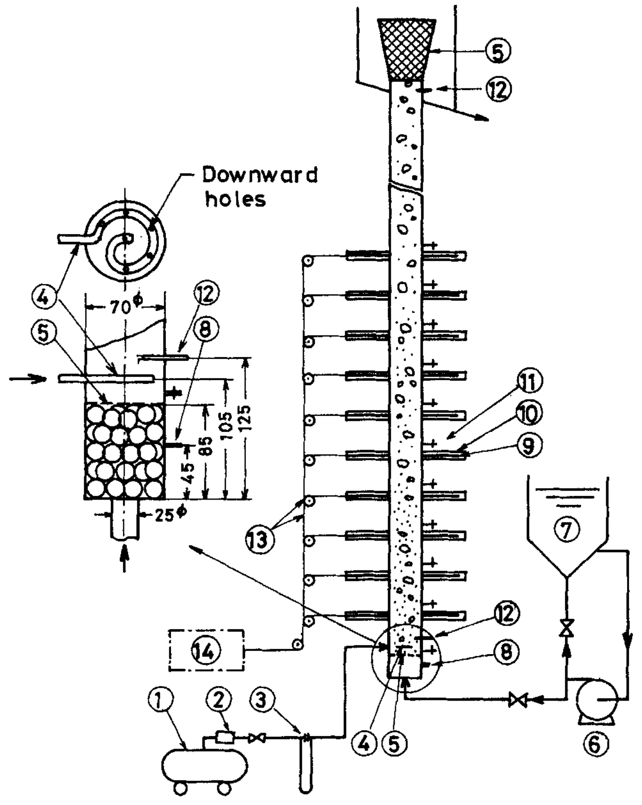


**Figure 1. Experimental apparatus.**

1. Compressor
2. Oil-mist separator
3. Orifice meter
4. Gas distributor
5. Bronze net
6. Pump
7. Reservoir
8. Tracer injection nozzle
9. Shutter plate
10. Shutter case
11. Solids withdrawal tap
12. Conductivity cell
13. Wire and pulley
14. Device for pulling wire

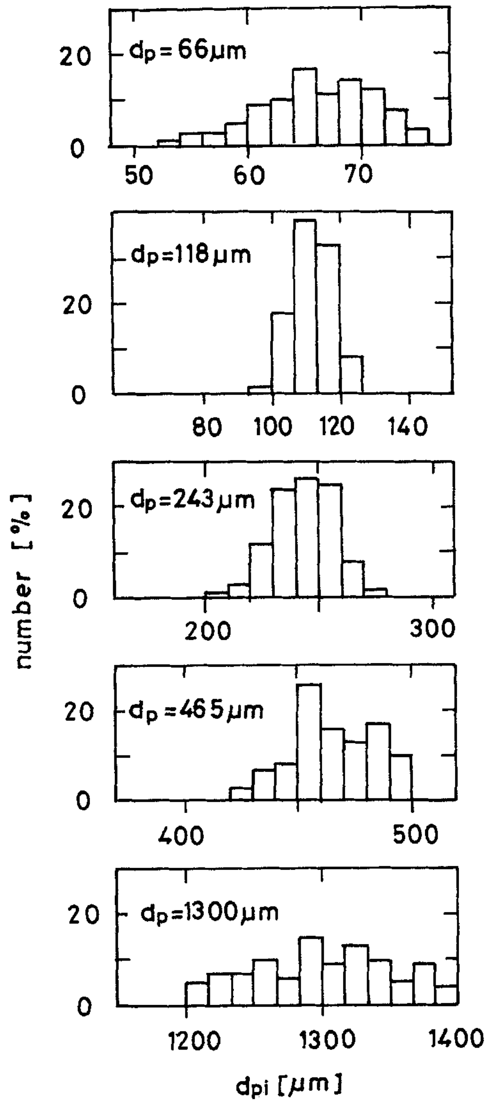


**Figure 2. Size distributions of glass beads used in experiment.**

response method described in previous works (Kago et al., 1988; Matsumoto et al., 1988).

## Results and Discussion

### *Gas holdup*

When the column is operated batchwise with respect to solid particles, the solid holdup can be kept constant throughout the column as shown in Figure 3, if certain combinations of gas and liquid flow rates are maintained. Figures 4 and 5 illustrate the mean gas holdup averaged over the column height under these circumstances. The effect of liquid velocity on the gas holdup for the solid-free gas-liquid system is taken into account by modifying the superficial gas velocity as $U_g(1 - R)$ where $R = [U_l/(1 - \epsilon_g)]/(U_g/\epsilon_g)$. Thus, the gas holdup for gas-liquid system is correlated by

$$\epsilon_g = U_g(1 - R)/[0.29 + 1.8\,U_g(1 - R)] \qquad (1)$$

In the case of $R = 0$, Eq. 1 is slightly smaller than the correlation of Kato and Nishiwaki (1971) and about 10% larger than that of Akita and Yoshida (1973).

For gas-liquid-solid systems, however, an appreciable decrease in gas holdup was observed with increasing solid holdup as indicated in Figures 4 and 5. The data with 118- and 234-$\mu$m particles are not plotted because the results are close to those for 465-$\mu$m particles. This means that the gas holdup is dependent on the solid holdup and not on the particle size. Based on these results, the gas holdup for gas-liquid-solid systems is represented by the following equation.

$$\epsilon_g = U_g(1 - R)/[0.29(1 + 2.5\phi_{p0}^{0.85}) + 1.8U_g(1 - R)] \qquad (2)$$

for $U_g = 0.01 - 0.3$ m · s$^{-1}$, $U_l = 0 - 0.15$ m · s$^{-1}$, $\phi_{p0} = 0 - 0.30$, $d_p = 66 - 1{,}300$ $\mu$m, and $R = 0 - 0.3$. Koide et al. (1984) proposed the following equation for the gas holdup in gas-liquid-solid bubble columns.

$$\frac{\epsilon_g}{(1 - \epsilon_g)^4} = \frac{0.277(U_g\eta/\sigma)^{0.918}\,[g\eta^4/(\rho_l\sigma^3)]^{-0.252}}{1 + 4.35\phi_{p0}^{0.748}\,[(\rho_p - \rho_l)/\rho_l]^{0.881}\,(D_TU_g\rho_l/\eta)^{-0.168}} \qquad (3)$$

Equation 3 underestimates the gas holdup at higher gas and liquid velocities, and does not contain the effect of liquid velocity.

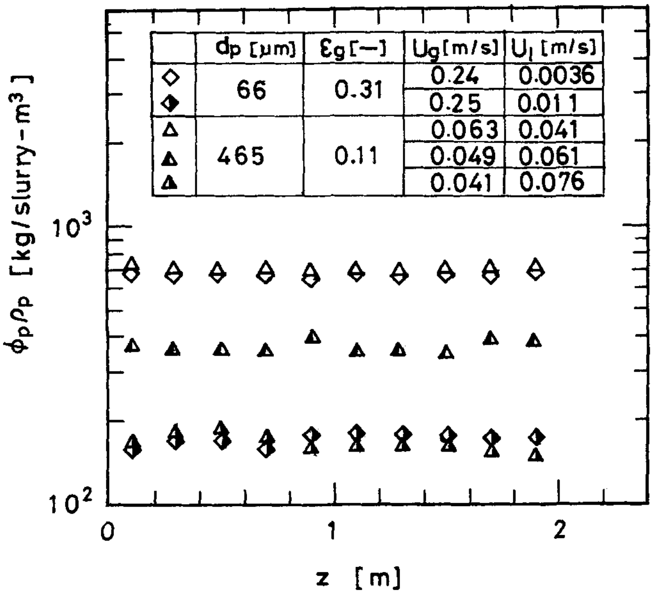


**Figure 3. Typical results of constant solid holdup runs.**

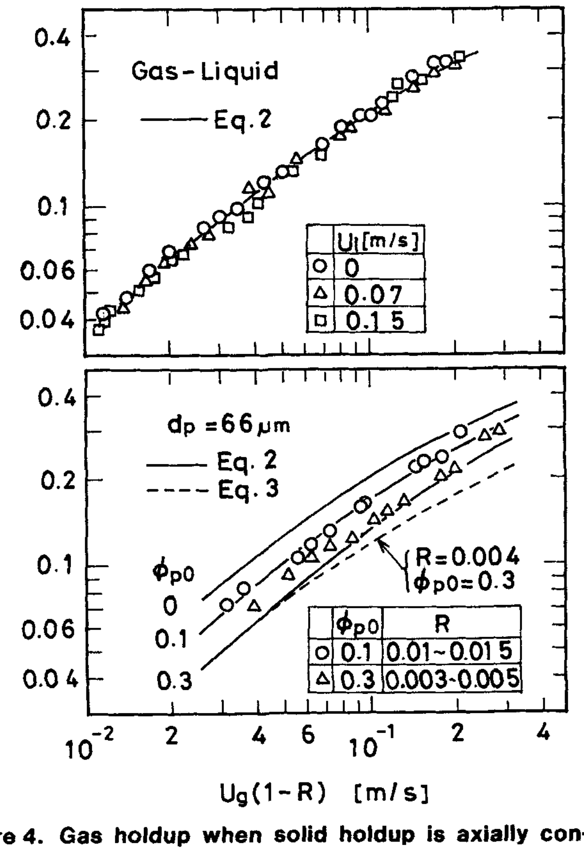


**Figure 4. Gas holdup when solid holdup is axially constant for gas-liquid system and $d_p$ = 66 $\mu$m.**

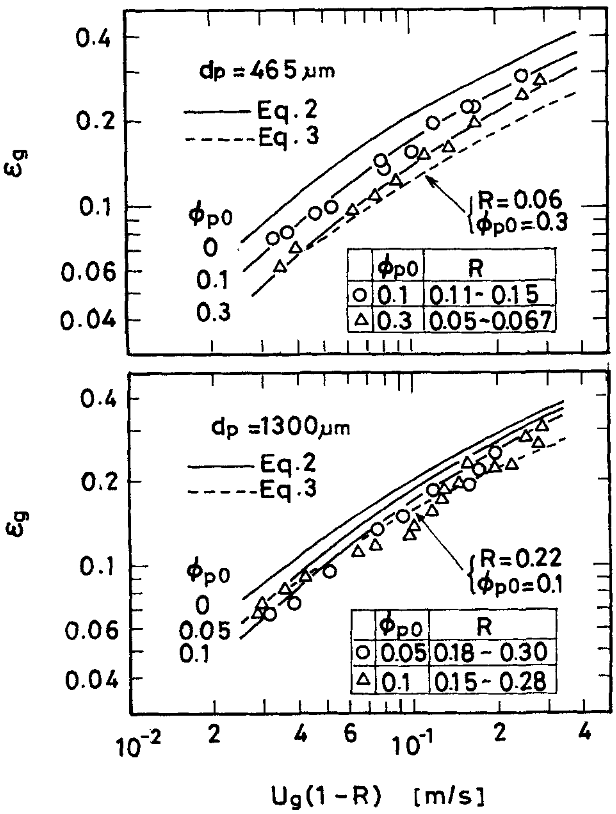


**Figure 5. Gas holdup when solid holdup is axially constant for $d_p$ = 465 and 1,300 $\mu$m.**

### *Settling velocity*

The local solid holdup in the slurry phase at the height $z$, $\phi_p$, is expressed by a one-dimensional dispersion model (Kato et al., 1972; Morooka et al., 1986; Smith and Ruether, 1985; Smith et al., 1986). For steady-state flow conditions,

$$\phi_p u_p - E_p d\phi_p/dz = \phi_{pf} U_{slf}/(1 - \epsilon_g) \tag{4}$$

$u_p$ is the linear solids velocity relative to the fixed coordinate and is related to the superficial liquid velocity and the effective settling velocity by the following equation (Garside and Al-Dibouni, 1977).

$$u_p = U_l/[(1 - \epsilon_g)(1 - \phi_p)] - v_\infty(1 - \phi_p)^{n-1} \tag{5}$$

The first term in the righthand side of Eq. 5 is the linear velocity of the liquid.

In the case of batch operation with respect to solids, $\phi_{pf} = 0$. Further, when $\phi_p$ is constant throughout the column ($= \phi_{p0}$) as shown in Figure 3, $d\phi_p/dz = 0$. Then $u_p = 0$ from Eq. 4, and Eq. 5 becomes

$$U_l/[(1 - \epsilon_g)(1 - \phi_{p0})] - v_\infty(1 - \phi_{p0})^{n-1} = 0 \tag{6}$$

Equation 6 corresponds to the expression of Richardson and Zaki (1954).

Figure 6 illustrates the relationship between the solid holdup and the liquid velocity when the solid holdup is controlled to be axially-constant. Data in the range of $(1 - \phi_{p0}) < 0.6$ are excluded because channeling flow of gas took place at higher solid holdups. The linear liquid velocity necessary to maintain the solid holdup at $\phi_{p0}$ increases with increasing $\epsilon_g$ and $(1 - \phi_{p0})$. This tendency is more evident with the smallest particles. The exponent $n$ is obtained from the slopes in Figure 6, and the effective settling velocity $v_\infty$ is determined from the intercept on the ordinate by extrapolating $(1 - \phi_{p0})$ to unity.

The values of $n$ for the gas-liquid-solid systems are not affected by the gas velocity in the range of the present experi-

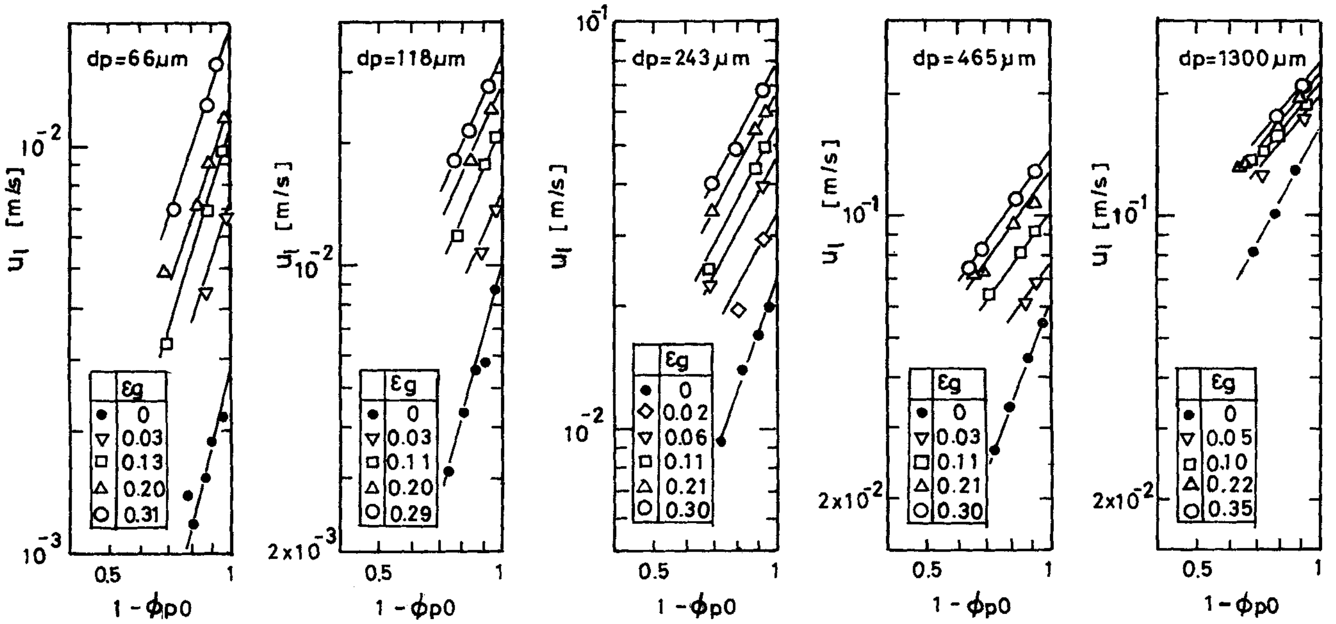

Figure 6. Relationship between $u_l$ and $(1 - \phi_{po})$ when solid holdup is axially constant.

ment and are correlated as a function of the Galilei number as shown in Figure 7.

$$(n - 2)/(5 - n) = 6.0Ga^{-1/2} \tag{7}$$

where $Ga = d_p^3 g(\rho_p/\rho_l - 1)/\nu^2$. The data for the liquid-solid system are in agreement with predictions by Garside and Al-Dibouni (1977), but are larger than the corresponding values determined using Eq. 7.

Figure 8 shows the correlation of $v_\infty$, which is dependent on the particle diameter and gas holdup. The abscissa of Figure 8 is the Galilei number modified by the gas holdup factor $\epsilon_g(1 - R)$. The effect of the column diameter on $v_\infty$ is negligible as reported by Kato et al. (1972) and Morooka et al. (1986).

The terminal velocity of a particle in quiescent liquid is normally expressed by Stokes', Allen's, and Newton's laws. To simplify the mathematical analysis, the following equation is adopted for the whole region with the maximum error of about 2%.

$$\frac{v_\infty d_p}{\nu} = \frac{Ga}{[18^{4/5} + (Ga/3.0)^{2/5}]^{5/4}} \tag{8}$$

Equation 8 gives the terminal velocity in the Newton's and Stokes' law regime if the first or second term in the denominator is neglected, respectively.

When a particle falls in the three-phase fluidized bed, however, the Galilei number in Eq. 8 must be corrected as

$$\frac{v_\infty d_p}{\nu} = \frac{Ga\zeta}{[18^{4/5} + (Ga\zeta/3.0)^{2/5}]^{5/4}} \tag{9}$$

$$\zeta = 1 + \left[\frac{6.5[\epsilon_g(1 - R)]^{1/2}Ga^{1/3}}{1 + [\{\epsilon_g(1 - R)\}^{1/2}Ga^{1/3}/15]^2}\right]^{3/2} Ga^{-2/3} \tag{10}$$

Figure 8 shows the comparison between experiment and calculation from Eqs. 9 and 10, as well as the correlation by Morooka et al. (1986) and Jean and Fan (1987). The estimation by Jean and Fan (1987) is lower than the present data for the 118-, 243- and 465-$\mu$m particles.

### Axial dispersion of liquid

Matsumoto et al. (1988) derived a mechanistic equation for $E_l$ on the basis of the mixing length theory. The overall energy balance in a three-phase column is:

(Work Done by Buoyant Force of Ascending Bubbles, $W_{gg}$)

$\doteqdot$ (Work Done by Turbulence Acting on Column Wall, $W_{lt}$) (11)

The work due to the interfacial energy and the viscous effect of the liquid is neglected. The lefthand term in Eq. 11 is given by:

$$W_{gg} = (\rho_{sl} - \rho_g)\,\epsilon_g g L'[\pi(D_T^2/4)L] \doteqdot \rho_{sl}\epsilon_g g L'[\pi(D_T^2/4)L] \tag{12}$$

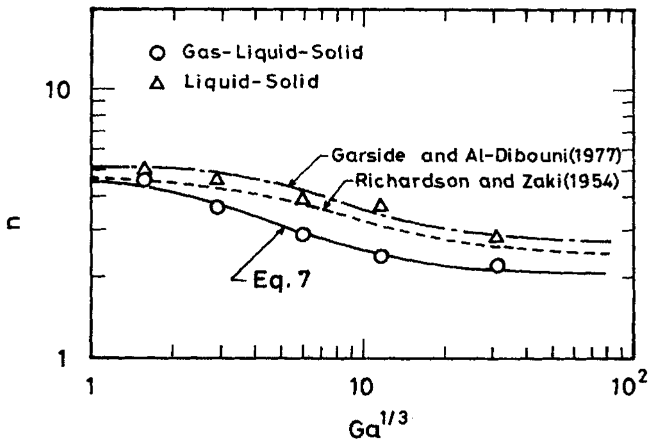


Figure 7. Correlation of exponent in Eq. 6.

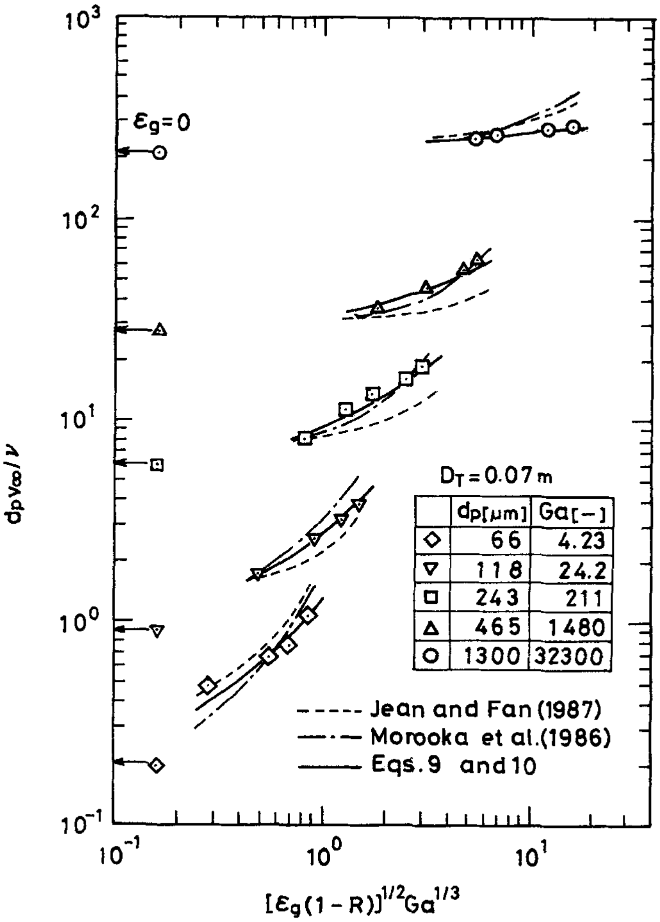


**Figure 8. Correlation of effective settling velocity of solids.**

where $L'$ is the effective distance, over which gas bubbles impose the buoyant force. As the mean residence time of ascending gas bubbles in the column decreases with increasing liquid velocity, $L'$ is written as

$$L' = (1 - R)L \tag{13}$$

Since the turbulent momentum flux in the slurry phase is $\rho_{sl}\overline{u_l'^2}$ per unit column wall area and per unit time, the small increment of $W_{lt}$ is given by

$$dW_{lt} = \rho_{sl}\overline{u_l'^2}(\pi D_T z)dz \tag{14}$$

Integrating Eq. 14 under the condition of $W_{lt} = 0$ at $z = 0$, we get

$$W_{lt} = \rho_{sl}\overline{u_l'^2}(L/2)(\pi D_T L) \tag{15}$$

By substituting Eqs. 12, 13 and 15 into Eq. 11, $\sqrt{\overline{u_l'^2}}$ is derived as

$$\sqrt{\overline{u_l'^2}} = [(1 - R)(gD_T/2)\epsilon_g]^{1/2} \tag{16}$$

The axial dispersion coefficient of liquid can be expressed by

$$E_l = l_l\sqrt{\overline{u_l'^2}} \tag{17}$$

where $l_l$ is given by Matsumoto et al. (1988) as follows:

$$l_l = k'D_T/(1 - \epsilon_g) \tag{18}$$

The denominator is introduced because the dispersion coefficient is defined on the basis of the slurry volume. Substituting $\sqrt{\overline{u_l'^2}}$ and $l_l$ into Eq. 17, we obtain

$$E_l = k[(1 - R)gD_T^3\epsilon_g]^{1/2}/(1 - \epsilon_g) \tag{19}$$

Matsumoto et al. (1988) elucidated that data of $E_l$ reported in the literature for different columns were correlated well by Eq. 19 using $k = 0.3$ for gas-liquid systems as shown in Figure 9 (Reith et al., 1968; Kato et al., 1971; Towell and Ackerman, 1972; Deckwer et al., 1974; Wachi et al., 1987). In the same figure, the present experimental results for gas-liquid systems are also plotted. Our data at higher liquid velocities are larger than those in the literature, indicating that $k$ is affected by the liquid velocity and resultantly by the gas holdup. Figure 10 shows that $k$ is represented well by using an empirical parameter $\epsilon_g U_l$. The dotted lines in Figures 9 and 10 are calculated from Eq. 19 with

$$k = 0.3[1 + 17.3(\epsilon_g U_l)^{3/4}] \tag{20}$$

### *Axial dispersion of solid particles*

The axial distribution of solid holdup for the batch operation with respect to solid particles is obtained by substituting Eq. 5 into Eq. 4 and with $\phi_{pf} = 0$.

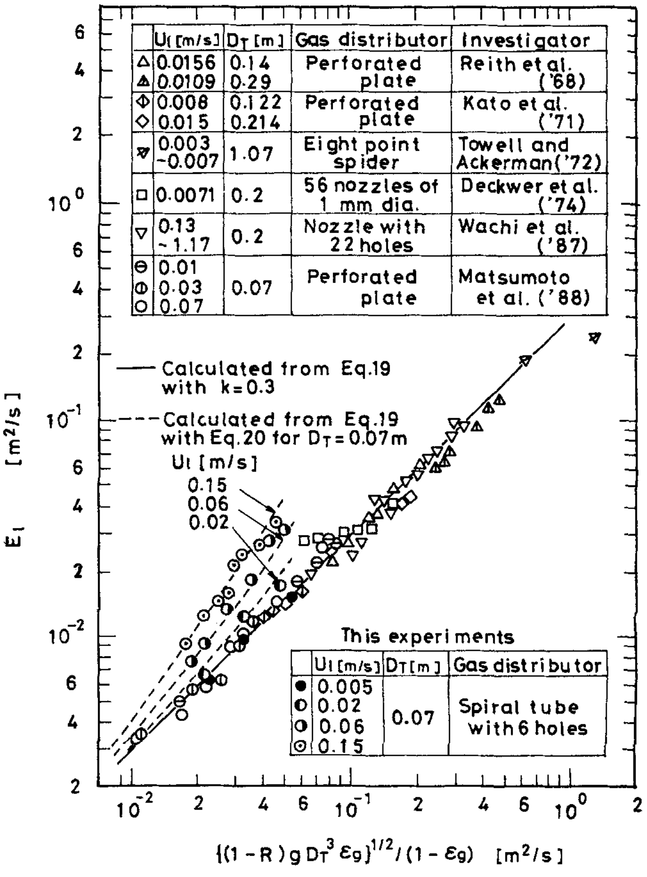


**Figure 9. Correlation of $E_l$ based on Eq. 19.**

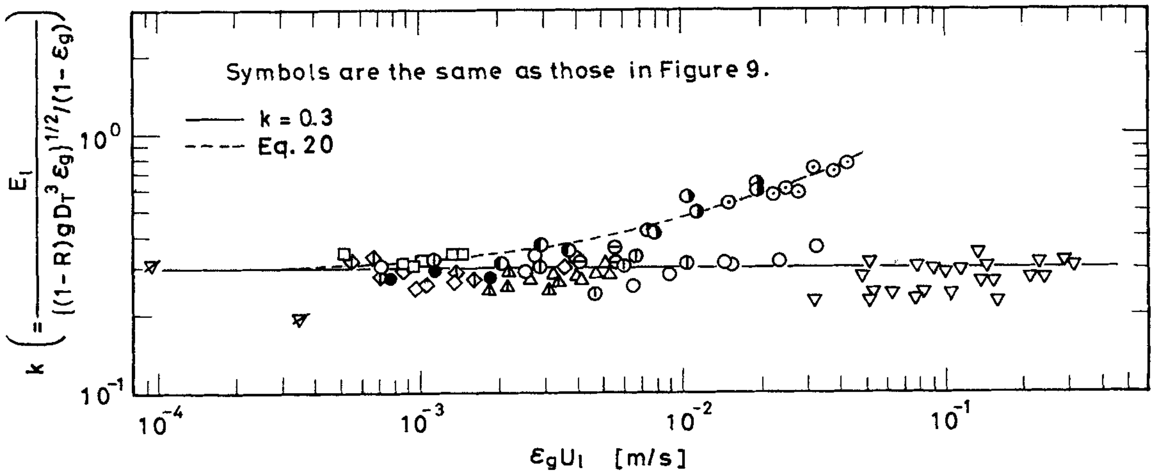


**Figure 10. Effects of gas holdup and liquid velocity on $E_l$.**

$$\left[\frac{U_l}{(1-\epsilon_g)(1-\phi_p)} - v_\infty(1-\phi_p)^{n-1}\right]\phi_p - E_p\frac{d\phi_p}{dz} = 0 \tag{21}$$

where the solid holdup is a function of the height, $z$. $E_p$ is assumed to be axially constant and is determined by comparing Eq. 21 with the measured concentration profile of solids. Figure 11 illustrates the axial distributions of solid holdup are described well by Eq. 21 in the range of $\phi_p = 0.02 - 0.3$. The values of $E_p$ as well as $E_l$ are plotted as a function of the mean value of $\epsilon_g$ in Figure 12. Evidently, $E_p$ is smaller than $E_l$ when larger particles are fluidized at a higher liquid velocity.

If $E_p$ is related to the turbulence in the same way as Eq. 17, $E_p/E_l$ is expressed by

$$E_p/E_l = (l_p\sqrt{\overline{u_p'^2}})/(l_l\sqrt{\overline{u_l'^2}}) \tag{22}$$

where $l_l$ and $l_p$ are the mixing length of liquid and solids, respectively. Since the mixing length in a bubble column is dominated by the motion of gas bubbles, we assume that $l_p = l_l$. Then Eq. 22 becomes

$$E_p/E_l = \sqrt{\overline{u_p'^2}}/\sqrt{\overline{u_l'^2}} \tag{23}$$

The root-mean-square velocity of solids, $\sqrt{\overline{u_p'^2}}$, is smaller than that of the liquid, because a certain relaxation time is needed for a particle to catch up with the liquid motion. If the particle size is smaller than the turbulence scale, the particle velocity relative to liquid can be described by the unsteady-state motion of a particle which is suddenly placed in a steady liquid flow of $v_l$. The equation of motion is given by the following equation in the dimensionless form (Dallavalle, 1942).

$$\frac{\rho_p}{\rho_l}\frac{d(v_p/v_l)}{dt^*} = (3/4)C_d(1 - v_p/v_l)^2 \tag{24}$$

where $t^* = tv_l/d_p$. The initial condition for Eq. 24 is

$$t = 0;\ v_p/v_l = 0 \tag{25}$$

The forces due to the pressure gradient in the liquid surrounding the particle and external potential such as gravity are negligible in comparison with the viscous force. In the intermediate region, the drag coefficient is given by Dallavalle (1948) as follows:

$$C_d = 0.4 + 40/[(1 - v_p/v_l)Re] \tag{26}$$

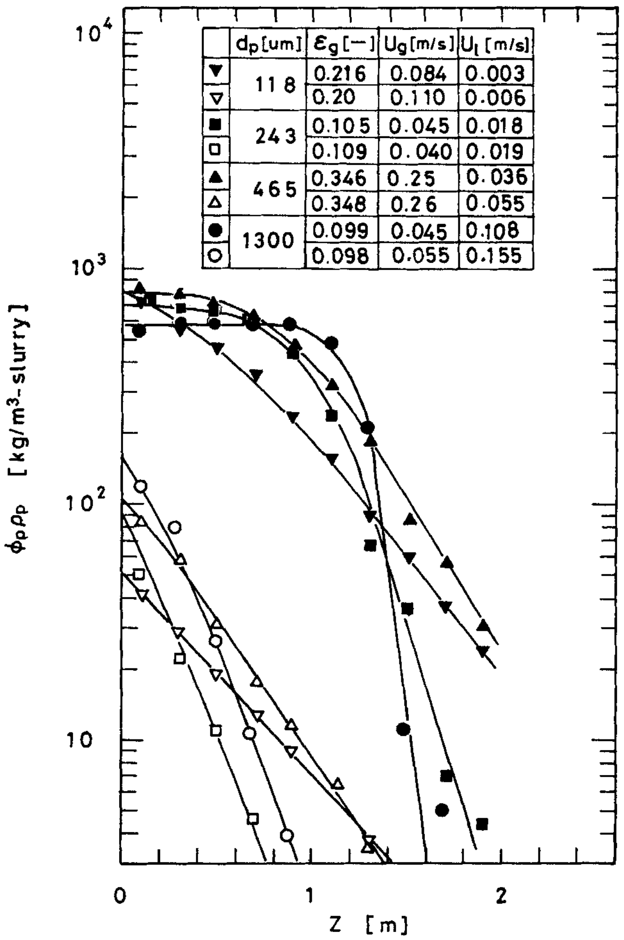


**Figure 11. Typical results of axial profiles of solid holdup.**

Solid lines are calculated from Eq. 21.

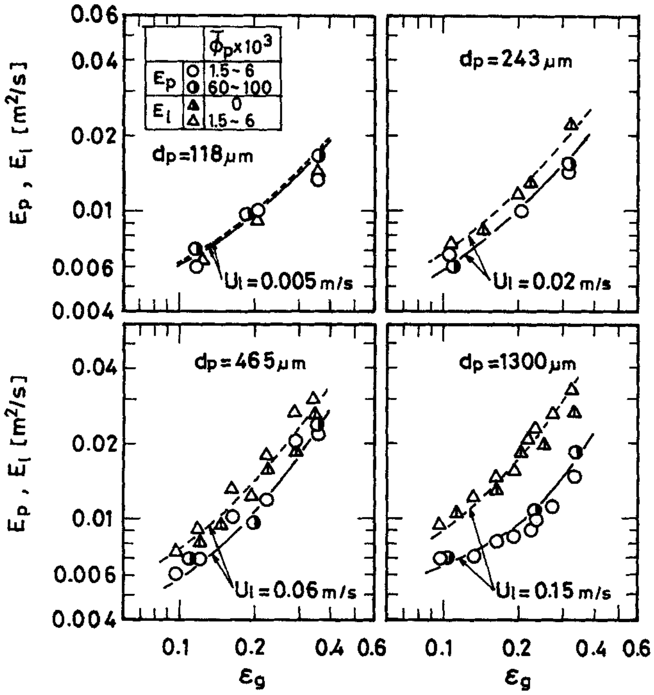


**Figure 12. Axial dispersion coefficient of solid particles and liquid.**

———, $E_p$ calculated from Eq. 29 with Eq. 19; – – – –, $E_l$ calculated from Eq. 19 with Eq. 20.

where $Re = d_p v_l/\nu$. This equation was adopted because of its simplicity in the integration. From Eqs. 24–26, the relative velocity of a particle at $t^*$ is obtained:

$$\frac{v_p}{v_l} = 1 - \frac{100/Re}{(1 + 100/Re)\exp[30t^*(\rho_l/\rho_p)/Re] - 1} \tag{27}$$

The time lag required to reach $v_p$ from $v_p = 0$ in a steady liquid flow is hypothetically characterized by the mixing time of liquid $l_l/\sqrt{\overline{u_l'^2}}$. Assuming $v_l = \sqrt{\overline{u_l'^2}}$, we get the following equation:

$$t^*\left(= \frac{tv_l}{d_p}\right) = K\frac{l_l}{\sqrt{\overline{u_l'^2}}}\frac{\sqrt{\overline{u_l'^2}}}{d_p} = K\frac{l_l\sqrt{\overline{u_l'^2}}}{\nu}\frac{\nu}{d_p\sqrt{\overline{u_l'^2}}} = K\frac{E_l}{\nu Re} \tag{28}$$

where $K$ is the correction factor for the turbulence scale and is determined experimentally. Substituting $v_p/v_l$ given by Eq. 27 for $\sqrt{\overline{u_p'^2}}/\sqrt{\overline{u_l'^2}}$ in Eq. 23, we obtain

$$\frac{E_p}{E_l} = 1 - \frac{100/Re}{(1 + 100/Re)\exp[30K(E_l/\nu)(\rho_l/\rho_p)/Re^2)] - 1} \tag{29}$$

The parameter $K$ in Eq. 29 is determined by comparing with the data and is correlated by

$$K = 0.04[1 + 1.8 \times 10^4\{d_p/[\epsilon_g(1 - R)]\}^2] \tag{30}$$

Equation 30 is valid for $\epsilon_g = 0.06 - 0.3$ and $d_p = 0.000066 - 0.0013$ m (the unit must be m). The liquid velocity in the Reynolds number used in Eq. 29 is transformed as follows:

$$Re = \frac{d_p v_l}{\nu} = \frac{d_p\sqrt{\overline{u_l'^2}}}{\nu} = \frac{d_p[(1 - R)(gD_T/2)\epsilon_g]^{1/2}}{\nu} \tag{31}$$

The last term was derived using Eq. 16. The calculated results of $E_p/E_l$ from Eqs. 29, 30 and 31 are shown in Figure 13. Further, $E_p$ is obtained by multiplying $E_p/E_l$ from Eqs. 29, 30 and 31 by $E_l$ from Eqs. 19 and 20, and the results are given in Figure 12 by the solid lines. The predictions are in good agreement with the experiments.

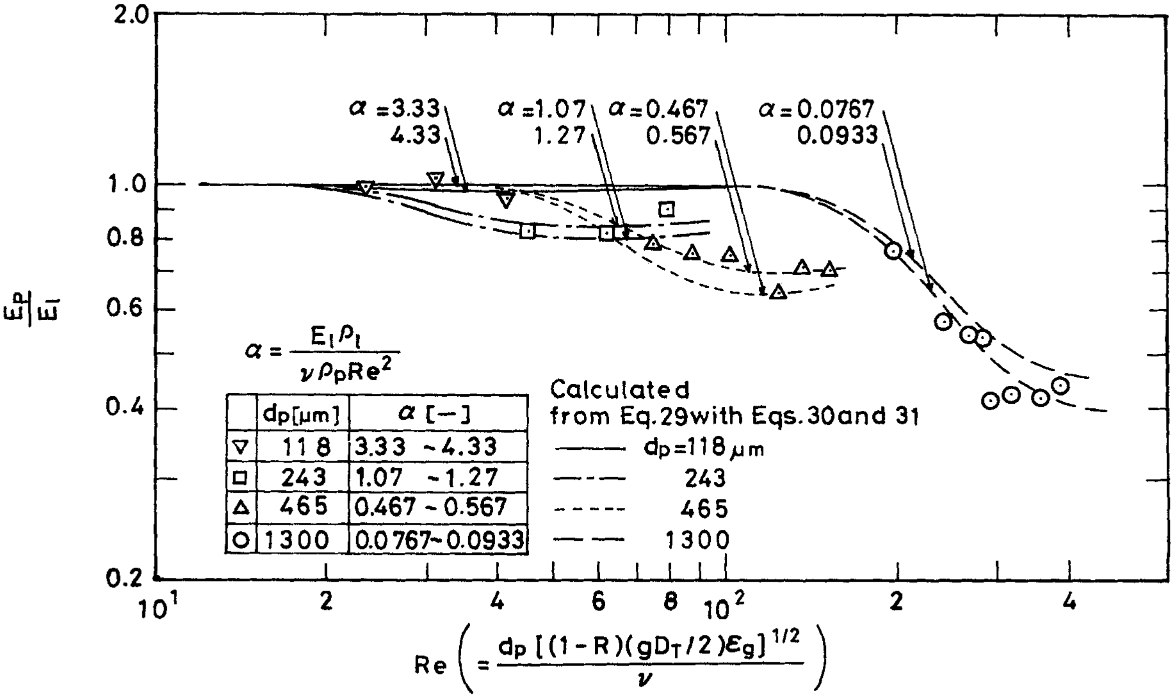


**Figure 13. Correlation of $E_p/E_l$.**

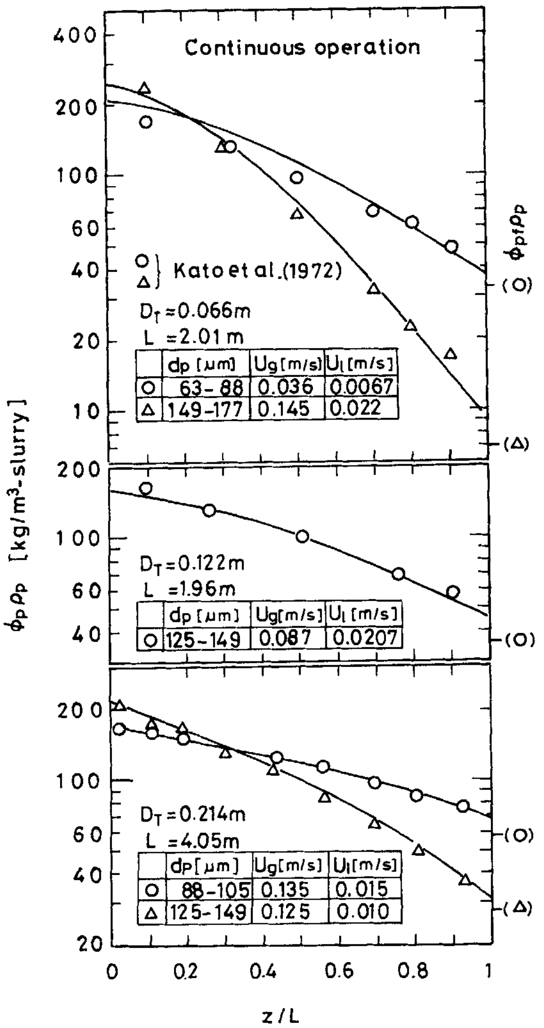


| | dp [μm] | Ug [m/s] | Ul [m/s] |
|---|---|---|---|
| O | 63- 88 | 0.036 | 0.0067 |
| Δ | 149-177 | 0.145 | 0.022 |

| | dp [μm] | Ug [m/s] | Ul [m/s] |
|---|---|---|---|
| O | 125-149 | 0.087 | 0.0207 |

| | dp [μm] | Ug [m/s] | Ul [m/s] |
|---|---|---|---|
| O | 88-105 | 0.135 | 0.015 |
| Δ | 125-149 | 0.125 | 0.010 |

**Figure 14. Simulation for axial changes of solid holdup for continuous operation.**
Solid lines are calculated from Eq. 4.

### *Simulated solid holdup profile in continuous operation*

The axial distribution of solid holdup with a solids feed ($\phi_{pf} \neq 0$) was analyzed with Eq. 4, whose parameters were estimated from Eqs. 2, 5, 19 and 29. Figure 14 shows the comparison between Eq. 4 and the experimental result of Kato et al. (1972). $E_l$ is calculated from Eq. 19 with $k = 0.30$, since their experiment was conducted at small liquid velocities with fine solid particles. Agreement is satisfactory. The experimental data of Smith and Ruether (1985) also agree with Eq. 4 (the result is not shown).

## Conclusions

- The effective settling velocity of solid particles in three-phase systems is described by Eq. 5 along with Eqs. 7, 9 and 10.
- The axial dispersion coefficient of liquid is correlated by Eqs. 19 and 20, while that of solid particles is given by Eqs. 29, 30 and 31.
- The axial distribution of solid holdup with and without solids feed is expressed by Eq. 4. General simulation of solid holdup profiles in a three-phase bubble column, which consists of the lower zone with a constant solids concentration and the upper zone with a decreasing solids concentration, has been satisfactorily elucidated for the first time as shown in Figures 11 and 14.

## Notation

$C$ = concentration of solid particles in slurry at $z$, kg/m³
$C_d$ = drag coefficient
$D_T$ = column diameter, m
$d_p$ = solid particle diameter, m
$E_l$ = axial dispersion coefficient of liquid, m²/s
$E_p$ = axial dispersion coefficient of solid particles, m²/s
$Ga$ = Galilei number defined by $dp^3 g(\rho_p/\rho_l - 1)/\nu^2$
$g$ = gravitational acceleration, m/s²
$K$ = correction factor defined by Eq. 28
$k$ = correction factor defined by Eq. 19
$k'$ = constant in Eq. 18
$L$ = height of column, m
$L'$ = effective height of column, m
$l_l$ = mixing length of liquid, m
$l_p$ = mixing length of solid particles, m
$n$ = exponent defined by Eq. 5
$R$ = dimensionless parameter defined by $\epsilon_g U_l/(1 - \epsilon_g)U_g$
$Re$ = Reynolds number
$t$ = time, s
$t^*$ = dimensionless time defined by $tv_l/d_p$
$U_{slf}$ = superficial slurry velocity in feed, m/s
$U_g$ = superficial gas velocity, m/s
$U_l$ = superficial liquid velocity, m/s
$u_l$ = linear liquid velocity, m/s
$u_l'$ = fluctuation liquid velocity, m/s
$u_p$ = linear solid particle velocity, m/s
$u_p'$ = fluctuation solid particle velocity, m/s
$v_l$ = steady-state liquid velocity used to calculate unsteady particle motion, m/s
$v_p$ = unsteady-state particle velocity, m/s
$v_\infty$ = effective settling velocity of solid particles in three-phase systems, equal to the terminal settling velocity of a particle in case of $U_g = 0$, m/s
$W_{gg}$, $W_{ll}$ = work defined by Eq. 11, J
$z$ = axial distance above gas distributor, m
$\bar{\ }$ = time smoothed

### *Greek letters*

$\epsilon_g$ = mean gas holdup averaged over the column height
$\zeta$ = correction factor defined by Eq. 9
$\eta$ = viscosity of liquid, Pa · s
$\nu$ = kinematic viscosity of liquid, m²/s
$\rho_l$ = density of liquid, kg/m³
$\rho_p$ = density of solid particles, kg/m³
$\rho_{sl}$ = density of slurry, kg/m³
$\sigma$ = surface tension, N/m
$\phi_p$ = solid holdup in slurry as a function of $z$, $C/\rho_p$
$\bar{\phi}_p$ = mean solid holdup in slurry averaged over the column height
$\phi_{p0}$ = $\phi_p$ which is kept constant throughout the column
$\phi_{pf}$ = $\phi_p$ in feed

## Literature Cited


Akita, K., and F. Yoshida, "Gas Holdup and Volumetric Mass Transfer Coefficient in Bubble Columns," *Ind. Eng. Chem. Proc. Des. Dev.*, **12**, 76 (1973).
Al-Dibouni, M. R., and J. Garside, "Particle Mixing and Classification in Liquid Fluidized Beds," *Trans IChemE.*, **57**, 94 (1979).
Dallavalle, J. M., *Micromeritics*, 2nd ed., Pitman, New York (1942).
Deckwer, W. D., R. Burckhart, and G. Zoll, "Mixing and Mass Transfer in Tall Bubble Columns," *Chem. Eng. Sci.*, **29**, 2177 (1974).
Fan, L.-S., T. Yamashita, and R. H. Jean, "Solid Mixing and Segregation in a Gas-Liquid-Solid Fluidized Bed," *Chem. Eng. Sci.*, **42**, 17 (1987).
Garside, J., and M. R. Al-Dibouni, "Velocity-Voidage Relationships for Fluidization in Solid-Liquid Systems," *Ind. Eng. Process Des. Dev.*, **16**, 206 (1977).

Imafuku, K., T. Y. Wang, K. Koide, and H. Kubota, "The Behavior of Suspended Solid Particles in the Bubble Column," *J. Chem. Eng. Japan*, **1**, 153 (1968).

Jean, R. H., and L.-S. Fan, "On the Particle Terminal Velocity in a Gas-Liquid Medium with Liquid as the Continuous Phase," *Can. J. Chem. Eng.*, **65**, 882 (1987).

Kago, T., Y. Sasaki, T. Kondo, S. Morooka, and Y. Kato, "Gas Holdup and Axial Dispersion of Gas and Liquid in Bubble Columns of Homogeneous Bubble Flow Regime," *Chem. Eng. Commun.*, **75**, 23 (1989).

Kato, Y., and A. Nishiwaki, "Longitudinal Dispersion Coefficient of Liquid in Bubble Column," *Kagaku Kogaku*, **35**, 912 (1971); *Int. Chem. Eng.*, **12**, 182 (1972).

Kato, Y., A. Nishiwaki, T. Fukuda, and S. Tanaka, "The Behavior of Suspended Solid Particles and Liquid in Bubble Columns," *J. Chem. Eng. Japan*, **5**, 112 (1972).

Kato, Y., S. Morooka, T. Kago, and S. Saruwatari, "Axial Holdup Distributions of Gas and Solid Particles in Three-Phase Fluidized Bed for Gas-Liquid (Slurry)-Solid Systems," *J. Chem. Eng. Japan*, **18**, 308 (1985).

Koide, K., A. Takazawa, M. Komura, and H. Matsunaga, "Gas Holdup and Volumetric Liquid-Phase Mass Transfer Coefficient in Solid-Suspended Bubble Columns," *J. Chem. Eng. Japan*, **17**, 459 (1984).

Matsumoto, T., N. Hidaka, H. Kamimura, M. Tsuchiya, T. Shimizu, and S. Morooka, "Turbulent Mixing-Length Model for Axial Turbulent Diffusion of Liquid in Three-Phase Fluidized Bed," *J. Chem. Eng. Japan*, **21**, 256 (1988).

Morooka, S., K. Kawazuishi, and Y. Kato, "Holdup and Flow Pattern of Solid Particles in Freeboard of Gas-Solid Fluidized Bed with Fine Particles," *Powder Technol.*, **26**, 75 (1980).

Morooka, S., T. Mizoguchi, T. Kago, Y. Kato, and N. Hidaka, "Effect of Fine Bubbles on Flow Properties in Bubble Column with Suspended Solid Particles," *J. Chem. Eng. Japan*, **19**, 507 (1986).

Reith, T., S. Renken, and A. Israel, "Gas Hold-up and Axial Mixing in the Fluid Phase of Bubble Columns," *Chem. Eng. Sci.*, **23**, 619 (1968).

Richardson, I. F., and W. N. Zaki, "Sedimentation and Fluidization: Part 1," *Trans. Inst. Chem. Engr.*, **32**, 35 (1954).

Smith, D. N., and J. A. Ruether, "Dispersed Solid Dynamics in a Slurry Bubble Column," *Chem. Eng. Sci.*, **40**, 741 (1985).

Smith, D. N., J. N. Ruether, Y. T. Shah, and M. N. Badgujar, "Modified Sedimentation-Dispersion Model for Solids in a Three-Phase Slurry Column," *AIChE J.*, **32**, 426 (Mar., 1986).

Towell, G. D., and G. H. Ackerman, "Axial Mixing of Liquid and Gas in Large Bubble Reactor," *Proc. Eur. Symp. Chem. Reaction Eng.*, **B3-1**, Elsevier, Amsterdam (1972).

Wachi, S., H. Morikawa, and K. Ueyama, "Gas Holdup and Axial Dispersion in Gas-Liquid Concurrent Bubble Column," *J. Chem. Eng. Japan*, **20**, 309 (1987).

*Manuscript received Jan. 23, 1989, and revision recieved June 26, 1989.*